A Simple and Analytical Parameter-Extraction Method of a Microwave MOSFET

Ickjin Kwon, *Student Member, IEEE*, Minkyu Je, *Student Member, IEEE*, Kwyro Lee, *Senior Member, IEEE*, and Hyungcheol Shin, *Senior Member, IEEE*

***Abstract*—A simple and accurate parameter-extraction method of a high-frequency small-signal MOSFET model including the substrate-related parameters and nonreciprocal capacitors is proposed. Direct extraction of each parameter using a linear regression approach is performed by Y-parameter analysis on the proposed equivalent circuit of the MOSFET for high-frequency operation. The extracted results are physically meaningful and good agreement has been obtained between the simulation results of the equivalent circuit and measured data without any optimization. Also, the extracted parameters, such as g_m and $g_{\rm ds}$, match very well with those obtained by dc measurement.**

***Index Terms*—CMOS, modeling, parameter extraction, microwave, small-signal equivalent circuit.**

I. Introduction

SMALL-SIGNAL modeling and parameter extraction of microwave transistors are not new issues. There are several well-established small-signal models, along with their related parameter-extraction methods for MESFETs, high electron-mobility transistors (HEMTs), and HBTs [1], [2]. However, CMOS now can operate at microwave frequencies. Although CMOS technology has many advantages over others, such as low cost, high integration, and the possibility of a single-chip solution, it is not easy to adapt the conventional small-signal models of compound semiconductors and parameter-extraction methods to CMOS devices. CMOS circuits are fabricated on a resistive substrate. To account for this difference, some parameters associated with substrate parasitics must be added to conventional models [3]–[7]. In addition, conventional models that allow simple direct extraction of parameters do not include a nonreciprocal capacitance, and this hurts their accuracy. Macro models were previously presented [3], a curve-fitting method for the extraction of the model elements was used [6], and nonreciprocal capacitance was not considered [7].

In this paper, we propose a simple, direct, and accurate parameter-extraction method for a small-signal MOSFET model including the substrate-related parameters and a complete set of nonreciprocal capacitors [8], [9]. This study focuses on a physics-based small-signal equivalent circuit of the microwave MOSFET and an accurate parameter-extraction approach by Y-parameter analysis from measured S-parameters. Our method can be considered an initial method of an optimization procedure for more complete models.

Manuscript received January 13, 2001. This work was supported by the Micro Information and Communication Remote Object-oriented Systems Research Center, Korea Advanced Institute of Science and Technology, and by the Korea Ministry of Science and Technology under the Tera-level Nanodevice Project.

The authors are with the Department of Electrical Engineering and Computer Science, Korea Advanced Institute of Science and Technology, Taejon 305-701, Korea (e-mail: ijkwon@mail.kaist.ac.kr).

Publisher Item Identifier S 0018-9480(02)05205-5.

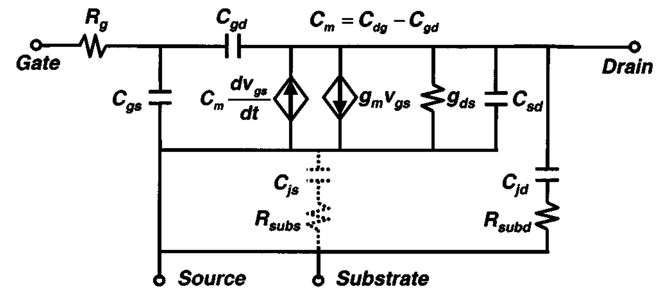

Fig. 1. Small-signal equivalent circuits of the MOSFET for microwave modeling. $C_{\rm js}$ and $R_{\rm subs}$ are excluded because the substrate is tied to the source. $C_m = C_{\rm dg} - C_{\rm gd}$ is a trans-capacitance taking care of the different effects of the gate and drain on each other.

II. Parameter-Extraction Method

We have proposed the small-signal equivalent circuit of a MOSFET for microwave modeling shown in Fig. 1. It is composed of physics-based parameters, including nonreciprocal capacitance and substrate-related parameters. The modeling and parameter extraction of a MOSFET with substrate-related parameter are much more complicated than that of a III–V FET. In this paper, we propose a direct extraction method of elements related to the substrate parameter for a three-terminal configuration. This model is suitable for the case of zero source-body bias in circuit. In a three-terminal configuration, $C_{\rm js}$ and $R_{\rm subs}$ are excluded because the substrate is tied to the source, as in most high-frequency applications.

Four intrinsic capacitances, i.e., $C_{\rm gs}, C_{\rm gd}, C_{\rm dg}$, and $C_{\rm sd}$, are required for the three-terminal model. The overlap capacitances are merged with the correspondent intrinsic capacitances.

$C_{\rm gd}$ and $C_{\rm dg}$ are the two nonreciprocal capacitance components for the three-terminal model [8]. The capacitive effect of the drain on the gate is represented by $C_{\rm gd}$, and the capacitive effect of the gate on the drain is represented by $C_{\rm dg}$. In general, $C_{\rm dg}$ is different from $C_{\rm gd}$. $C_m = C_{\rm dg} - C_{\rm gd}$ is a transcapacitance taking care of the different effects of the gate and the drain on each other in terms of charging currents. Similarly, g_m is a transconductance taking care of the different effects of these two terminals on each other in terms of transport currents [9]. If $C_{\rm gd}$ and $C_{\rm dg}$ are set to be equal, as in most conventional models, a large error may be introduced since charge conservation does not hold. In the ac simulation, the transcapacitance has to be included for accurate prediction of transadmittances Y_{21} and Y_{12}.

Without nonreciprocal gate–drain capacitance, it is impossible to model $\mathrm{Im}[Y_{21}]$ and $\mathrm{Im}[Y_{12}]$ accurately at the same time. In the case of a four-terminal model with separate substrate terminals, a similar approach can be extended by including other nonreciprocal capacitances.

The resistance R_g represents the effective gate resistance that consists of the distributed channel resistance and the gate electrode resistance [10]. These effects are approximated by a single effective lumped gate resistance, as shown in the equivalent circuit of the MOSFET shown in Fig. 1. For simplicity and ease of extraction, source–drain resistances were not included in the model. Omitting source–drain resistances will have a slight effect on R_g and g_m values. However, these extracted R_g and g_m are adequate for fitting network parameters and can also be used as initial values for further optimization. R_g significantly affects the input admittance Y_{11} at high frequency. The drain junction capacitance and the bulk spreading resistance are represented by C_{jd} and R_{subd}, respectively. As the operation frequency increases, the impedance of the junction capacitance reduces. Thus, the substrate coupling effects through the drain junction and substrate resistance become significant for the output admittance Y_{22}. The parasitic inductances were not included since their effects are small up to 10 GHz.

Direct extraction using a linear-regression approach is performed by Y-parameter analysis on the equivalent circuit of the MOSFET for high-frequency operation. In our approach, an optimization process, which may have uncertainties in obtaining physical parameters, is not required. The small-signal equivalent circuit shown in Fig. 1 can be analyzed in terms of Y-parameters as follows:

$$\begin{aligned}Y_{11} &= \left.\frac{I_1}{V_1}\right|_{V_2=0} = \frac{j\omega(C_{\mathrm{gs}}+C_{\mathrm{gd}})}{1+j\omega(C_{\mathrm{gs}}+C_{\mathrm{gd}})R_g}\\ &= \frac{\omega^2(C_{\mathrm{gs}}+C_{\mathrm{gd}})^2R_g+j\omega(C_{\mathrm{gs}}+C_{\mathrm{gd}})}{1+\omega^2(C_{\mathrm{gs}}+C_{\mathrm{gd}})^2R_g^2}\end{aligned} \tag{1}$$

$$\begin{aligned}Y_{12} &= \left.\frac{I_1}{V_2}\right|_{V_1=0} = \frac{-j\omega C_{\mathrm{gd}}}{1+j\omega(C_{\mathrm{gs}}+C_{\mathrm{gd}})R_g}\\ &= \frac{-\omega^2C_{\mathrm{gd}}(C_{\mathrm{gs}}+C_{\mathrm{gd}})R_g-j\omega C_{\mathrm{gd}}}{1+\omega^2(C_{\mathrm{gs}}+C_{\mathrm{gd}})^2R_g^2}\end{aligned} \tag{2}$$

$$\begin{aligned}Y_{21} &= \left.\frac{I_2}{V_1}\right|_{V_2=0} = \frac{g_m-j\omega C_m-j\omega C_{\mathrm{gd}}}{1+j\omega(C_{\mathrm{gs}}+C_{\mathrm{gd}})R_g} = \frac{g_m-j\omega C_{\mathrm{dg}}}{1+j\omega(C_{\mathrm{gs}}+C_{\mathrm{gd}})R_g}\\ &= \frac{g_m-\omega^2C_{\mathrm{dg}}(C_{\mathrm{gs}}+C_{\mathrm{gd}})R_g-j\omega C_{\mathrm{dg}}-j\omega g_mR_g(C_{\mathrm{gs}}+C_{\mathrm{gd}})}{1+\omega^2(C_{\mathrm{gs}}+C_{\mathrm{gd}})^2R_g^2}\end{aligned} \tag{3}$$

$$\begin{aligned}Y_{22} &= \left.\frac{I_2}{V_2}\right|_{V_1=0}\\ &= g_{\mathrm{ds}}+\frac{j\omega C_{\mathrm{jd}}}{1+j\omega C_{\mathrm{jd}}R_{\mathrm{subd}}}+j\omega C_{\mathrm{sd}}+j\omega C_{\mathrm{gd}} + \frac{\omega^2C_{\mathrm{gd}}R_g(C_{\mathrm{gd}}+C_m)+j\omega g_mC_{\mathrm{gd}}R_g}{1+j\omega(C_{\mathrm{gs}}+C_{\mathrm{gd}})R_g}\\ &= g_{\mathrm{ds}}+\frac{j\omega C_{\mathrm{jd}}}{1+j\omega C_{\mathrm{jd}}R_{\mathrm{subd}}} +j\omega C_{\mathrm{sd}}+j\omega C_{\mathrm{gd}} + \frac{\omega^2C_{\mathrm{gd}}C_{\mathrm{dg}}R_g+j\omega g_mC_{\mathrm{gd}}R_g}{1+j\omega(C_{\mathrm{gs}}+C_{\mathrm{gd}})R_g}\\ &= g_{\mathrm{ds}}+\frac{\omega^2C_{\mathrm{jd}}^2R_{\mathrm{subd}}}{1+\omega^2C_{\mathrm{jd}}^2R_{\mathrm{subd}}^2} + \frac{\omega^2C_{\mathrm{gd}}C_{\mathrm{dg}}R_g+\omega^2g_mR_g^2C_{\mathrm{gd}}(C_{\mathrm{gs}}+C_{\mathrm{gd}})}{1+\omega^2(C_{\mathrm{gs}}+C_{\mathrm{gd}})^2R_g^2}\\ &\quad + \frac{j\omega C_{\mathrm{jd}}}{1+\omega^2C_{\mathrm{jd}}^2R_{\mathrm{subd}}^2}+j\omega C_{\mathrm{sd}}+j\omega C_{\mathrm{gd}} + \frac{j\omega g_mR_gC_{\mathrm{gd}}-j\omega^3C_{\mathrm{gd}}C_{\mathrm{dg}}(C_{\mathrm{gs}}+C_{\mathrm{gd}})R_g^2}{1+\omega^2(C_{\mathrm{gs}}+C_{\mathrm{gd}})^2R_g^2}.\end{aligned} \tag{4}$$

For operation frequency up to 10 GHz, by using the assumption that $\omega^2(C_{\mathrm{gs}}+C_{\mathrm{gd}})^2R_g^2 \ll 1$, the Y-parameters can be approximated as follows:

$$Y_{11} \approx \omega^2(C_{\mathrm{gs}}+C_{\mathrm{gd}})^2R_g+j\omega(C_{\mathrm{gs}}+C_{\mathrm{gd}}) \tag{5}$$

$$Y_{12} \approx -\omega^2C_{\mathrm{gd}}(C_{\mathrm{gs}}+C_{\mathrm{gd}})R_g-j\omega C_{\mathrm{gd}} \tag{6}$$

$$\begin{aligned}Y_{21} &\approx g_m-\omega^2C_{\mathrm{dg}}(C_{\mathrm{gs}}+C_{\mathrm{gd}})R_g\\ &\quad -j\omega C_{\mathrm{dg}}-j\omega g_mR_g(C_{\mathrm{gs}}+C_{\mathrm{gd}})\end{aligned} \tag{7}$$

$$\begin{aligned}Y_{22} &\approx g_{\mathrm{ds}}+\frac{\omega^2C_{\mathrm{jd}}^2R_{\mathrm{subd}}}{1+\omega^2C_{\mathrm{jd}}^2R_{\mathrm{subd}}^2}+\omega^2C_{\mathrm{gd}}C_{\mathrm{dg}}R_g\\ &\quad +\omega^2g_mR_g^2C_{\mathrm{gd}}(C_{\mathrm{gs}}+C_{\mathrm{gd}})\\ &\quad +\frac{j\omega C_{\mathrm{jd}}}{1+\omega^2C_{\mathrm{jd}}^2R_{\mathrm{subd}}^2}+j\omega C_{\mathrm{sd}}+j\omega C_{\mathrm{gd}}+j\omega g_mR_gC_{\mathrm{gd}}\\ &\quad -j\omega^3C_{\mathrm{gd}}C_{\mathrm{dg}}(C_{\mathrm{gs}}+C_{\mathrm{gd}})R_g^2.\end{aligned} \tag{8}$$

The validity of the assumption that $\omega^2(C_{\mathrm{gs}}+C_{\mathrm{gd}})^2R_g^2 \ll 1$ will be checked after each parameter is extracted. All the components of the equivalent circuit are extracted by the Y-parameter analysis and analytical equations are derived from real and imaginary parts of the Y-parameters. g_m is obtained from the y-intercept of $\mathrm{Re}[Y_{21}]$ versus ω^2 and g_{ds} is extracted from the y-intercept of $\mathrm{Re}[Y_{22}]$ versus ω^2 at the low frequency range. R_g, C_{gd}, C_{gs}, and C_{dg} can be obtained by (11)–(14) as follows:

$$g_m = \mathrm{Re}[Y_{21}]\,|_{\omega^2=0} \tag{9}$$

$$g_{\mathrm{ds}} = \mathrm{Re}[Y_{22}]\,|_{\omega^2=0} \tag{10}$$

$$R_g = \mathrm{Re}[Y_{11}]/(\mathrm{Im}[Y_{11}])^2 \tag{11}$$

$$C_{\mathrm{gd}} = -\mathrm{Im}[Y_{12}]/\omega \tag{12}$$

$$C_{\mathrm{gs}} = (\mathrm{Im}[Y_{11}]+\mathrm{Im}[Y_{12}])/\omega \tag{13}$$

$$C_{\mathrm{dg}} = -\mathrm{Im}[Y_{21}]/\omega - g_mR_g(C_{\mathrm{gs}}+C_{\mathrm{gd}}). \tag{14}$$

For the extraction of substrate components, $R_{\rm subd}$ and $C_{\rm jd}, Y_{\rm sub}$ is first defined as follows:

$$\begin{aligned} Y_{\rm sub} &= Y_{22} - g_{\rm ds} - \omega^2 C_{\rm gd} C_{\rm dg} R_g - \omega^2 g_m R_g^2 C_{\rm gd} \\ &\quad \times (C_{\rm gs} + C_{\rm gd}) - j\omega C_{\rm sd} - j\omega C_{\rm gd} - j\omega g_m R_g C_{\rm gd} \\ &\quad + j\omega^3 C_{\rm gd} C_{\rm dg} (C_{\rm gs} + C_{\rm gd}) R_g^2 \\ &= \frac{\omega^2 C_{\rm jd}^2 R_{\rm subd}}{1 + \omega^2 C_{\rm jd}^2 R_{\rm subd}^2} + \frac{j\omega C_{\rm jd}}{1 + \omega^2 C_{\rm jd}^2 R_{\rm subd}^2}. \end{aligned} \tag{15}$$

$R_{\rm subd}$ is obtained from the slope of the relationship for $\omega^2/{\rm Re}[Y_{\rm sub}]$ versus ω^2 by (16) as follows:

$$\frac{\omega^2}{{\rm Re}[Y_{\rm sub}]} = \omega^2 R_{\rm subd} + \frac{1}{C_{\rm jd}^2 R_{\rm subd}}. \tag{16}$$

$C_{\rm jd}$ is obtained from (17) as follows:

$$C_{\rm jd} = \left(\frac{\omega^2 R_{\rm subd}}{{\rm Re}[Y_{\rm sub}]} - \omega^2 {R_{\rm subd}}^2 \right)^{-1/2}. \tag{17}$$

Finally, $C_{\rm sd}$ is obtained from (8) as

$$\begin{aligned} C_{\rm sd} = \frac{{\rm Im}[Y_{22}]}{\omega} - C_{\rm gd} - \frac{C_{\rm jd}}{1 + \omega^2 C_{\rm jd}^2 R_{\rm subd}^2} \\ - g_m R_g C_{\rm gd} + \omega^2 C_{\rm gd} C_{\rm dg} (C_{\rm gd} + C_{\rm gs}) R_g^2. \end{aligned} \tag{18}$$

III. Experiments and Results

The proposed direct extraction method was applied to determine the parameters of the test devices, which were multifingered n-MOSFETs fabricated by 0.35-μm technology. S-parameters are measured in the common source–substrate configuration using on-wafer RF probes and an HP 8510C vector network analyzer. The initial calibration was performed on a separate ceramic calibration substrate using a SOLT calibration method. Before the extraction process, parasitic components of input and output pads have to be removed. To remove on-wafer pad parasitics, a deembedding technique was carried out by subtracting Y-parameters of the open pad structure from Y-parameters of the measured device. The parameter extraction has been performed for an n-MOSFET with 100-μm width having 20-unit gate fingers. All the small-signal parameters were extracted using (9)–(18).

Fig. 2 shows the extraction results of conductances g_m and $g_{\rm ds}$ at $V_{\rm gs} = 1$ V and $V_{\rm ds} = 2$V. Transconductance g_m of 16.6 mS was obtained from the Y-intercept of ${\rm Re}[Y_{21}]$ versus ω^2, as shown in Fig. 2(a), and the conductance $g_{\rm ds}$ of 0.31 mS was extracted from the intercept of ${\rm Re}[Y_{22}]$ versus ω^2, at the low-frequency range, as shown in Fig. 2(b). In Fig. 3, $\omega^2/{\rm Re}[Y_{\rm sub}]$ is linearly proportional to ω^2 and $R_{\rm subd}$ of 191 Ω was determined from the slope.

In Fig. 4, the frequency dependence of extracted parameters such as $R_g, C_{\rm gd}, C_{\rm gs}, C_{\rm dg}, C_{\rm jd}$, and $C_{\rm sd}$ at $V_{\rm gs} = 1$ V and $V_{\rm ds} = 2$ V are shown. The results show that the extracted parameters remain almost constant with frequency. This verifies that those components are frequency independent and the proposed

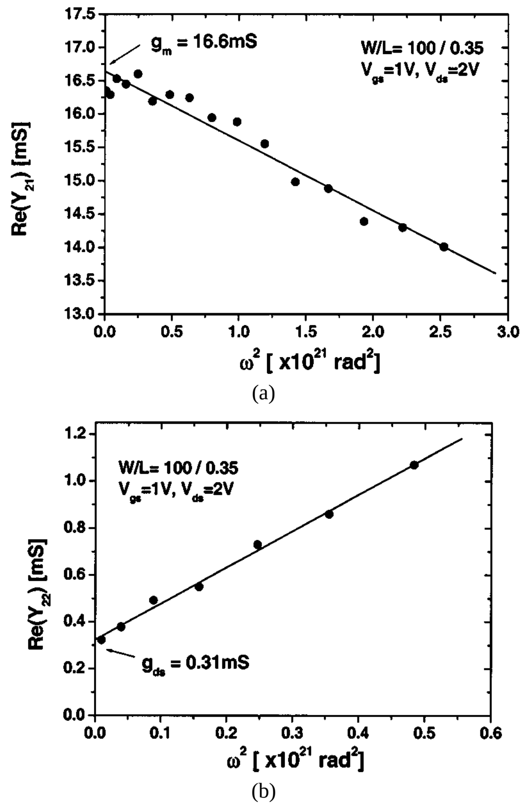

Fig. 2. Extraction results of conductances g_m and $g_{\rm ds}$. (a) g_m were obtained from the Y-intercept of ${\rm Re}[Y_{21}]$ versus ω^2. (b) $g_{\rm ds}$ was extracted from the intercept of ${\rm Re}[Y_{22}]$ versus ω^2 at the low-frequency range.

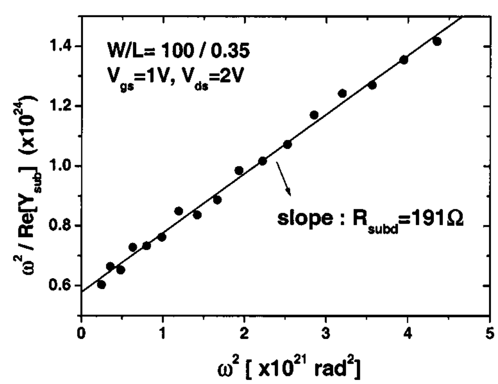

Fig. 3. $R_{\rm subd}$ was determined from the slope of $\omega^2/{\rm Re}[Y_{\rm sub}]$ as a function of ω^2.

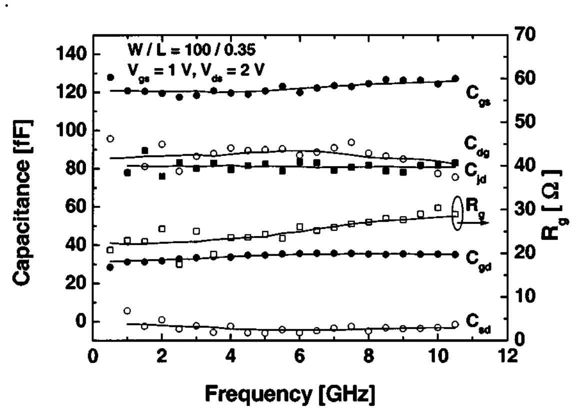

Fig. 4. Frequency dependence of extracted parameters for an n-MOSFET having 100-μm width and biased to $V_{\rm gs} = 1$ V and $V_{\rm ds} = 2$ V. Extracted parameters remain almost constant with frequency, verifying that the method is accurate and reliable.

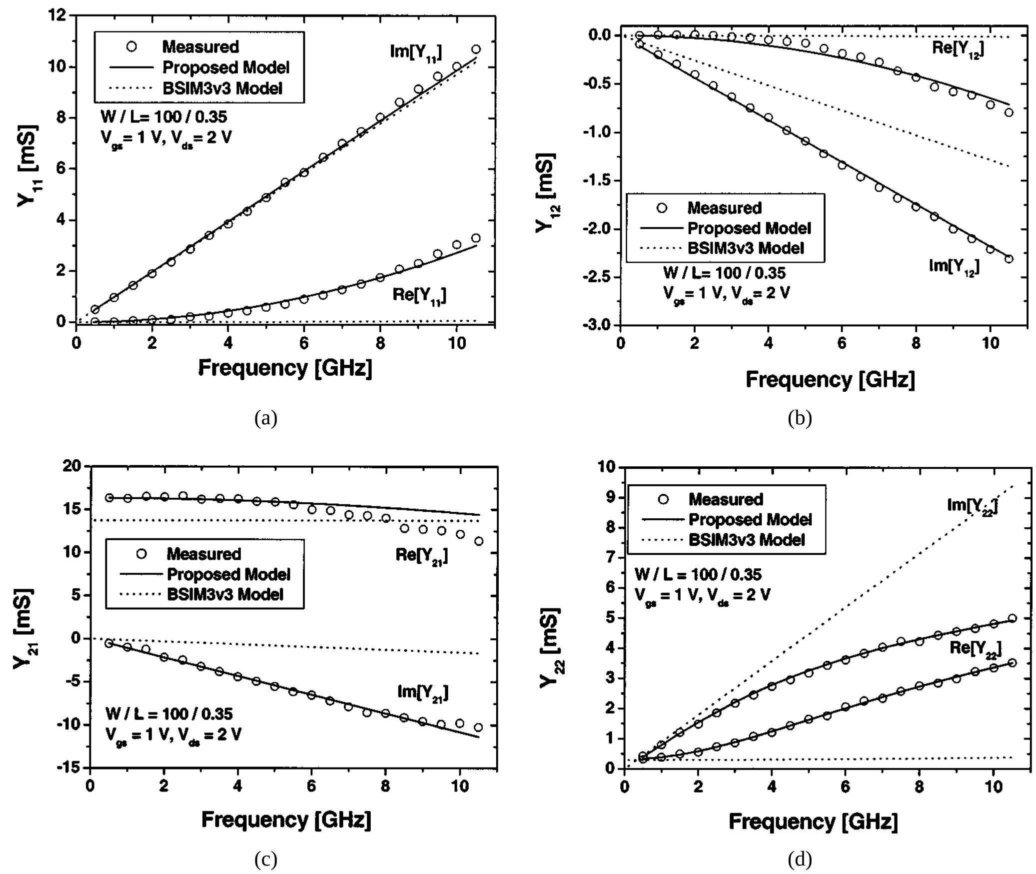

Fig. 5. Y-parameters of measurement (symbol), proposed model (solid line), and BSIM3v3 model (dotted line) for the n-MOSFET biased to $V_{\rm gs} = 1$ V and $V_{\rm ds} = 2$ V. (a) Y_{11}. (b) Y_{12}. (c) Y_{21}. (d) Y_{22}. The frequency range is from 0.5 to 10.5 GHz. The simulated results with the proposed model match the measured Y-parameters very well without any optimization after parameter extraction.

TABLE I
AVERAGE VALUES OF THE EXTRACTED PARAMETERS FOR AN n-MOSFET HAVING 100-μm WIDTH AND BIASED TO $V_{\rm gs} = 1$ V AND $V_{\rm ds} = 2$ V

g_m	16.6 mS
g_{ds}	0.31 mS
R_g	25.3 Ω
C_{gd}	34 fF
C_{gs}	122.4 fF
C_{dg}	86 fF
R_{subd}	191Ω
C_{jd}	81.1 fF
C_{sd}	-3.1 fF

extraction method is accurate and reliable. Due to the nonreciprocity, $C_{\rm dg}$ is larger than $C_{\rm gd}$. For the extracted parameter values, $\omega^2(C_{\rm gs} + C_{\rm gd})^2 R_g^2$ is calculated to be 0.055, even at 10 GHz, which is much smaller than one. This verifies the validity of using the assumption in simplifying (1)–(4) to (5)–(8). The average values of the extracted parameters are summarized in Table I.

In Fig. 5, the simulation results for Y-parameters obtained by using the equivalent circuit shown in Fig. 1 with extracted values are compared with the measured data for $V_{\rm gs} = 1$ V and $V_{\rm ds} = 2$ V. The proposed model is also compared with the BSIM3v3 model. It shows that the simulation results matched well with the measurements without any optimization after parameter extraction. The proposed model is more accurate than the BSIM3v3 model, as shown in Fig. 5. The nonreciprocal capacitances $C_{\rm gd}$ and $C_{\rm dg}$ contribute to match ${\rm Im}[Y_{12}]$ and ${\rm Im}[Y_{21}]$. Excluding transcapacitance could result in a significant error on ${\rm Im}[Y_{21}]$ at high frequency. The substrate coupling significantly contributes to the real part of the output admittance Y_{22} at high frequency. The discrepancy observed in ${\rm Re}[Y_{21}]$ between the measured and modeled data, as shown in Fig. 5(c), is probably because ${\rm Re}[Y_{21}]$ data were not used in our parameter extraction. The total error [11] between measured and simulated Y-parameters of the proposed model calculated as follows by (19) is only 0.4%:

$$\varepsilon_{\rm tot}(Y) = 100 \cdot \frac{1}{4} \cdot \sum_{ij} \left\{ \sum_{\rm freq} \frac{\left| {\rm meas}Y_{ij} - {\rm sim}Y_{ij} \right|^2}{\left| {\rm meas}Y_{ij} \right|^2} \right\} \frac{1}{N_{\rm freq}}. \tag{19}$$

The total error in the S-parameter calculated as follows by (20) is 0.18%:

$$\varepsilon_{\rm tot}(S) = 100 \cdot \frac{1}{4} \cdot \sum_{ij} \left\{ \sum_{\rm freq} \frac{\left| {\rm meas}S_{ij} - {\rm sim}S_{ij} \right|^2}{\left| {\rm meas}S_{ij} \right|^2} \right\} \frac{1}{N_{\rm freq}}. \tag{20}$$

In Fig. 6, gate-bias dependences of the extracted small-signal parameters for the n-MOSFET biased to $V_{\rm ds} = 2$ V are shown.

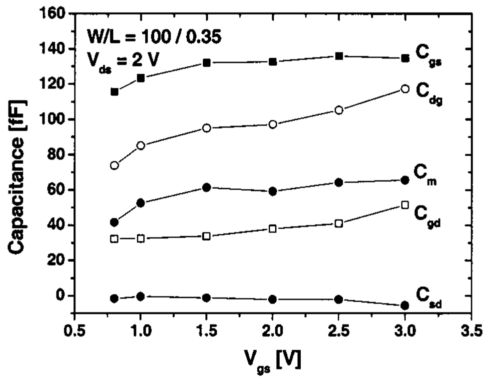

(a)

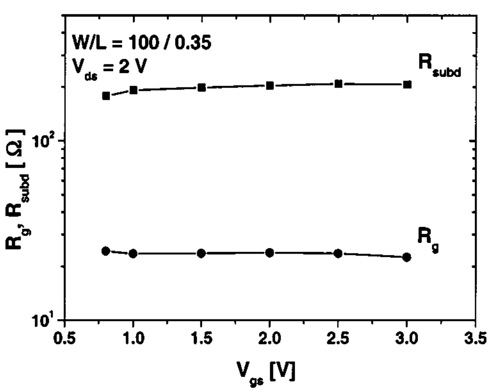

(b)

Fig. 6. Gate-bias dependence of small-signal parameters for an n-MOSFET having 100-μm width and biased to $V_{\rm ds} = 2$ V. (a) Capacitances. (b) R_g and $R_{\rm subd}$.

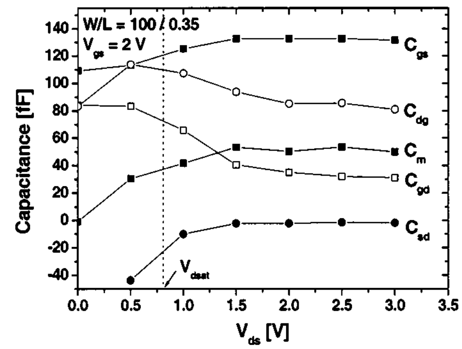

(a)

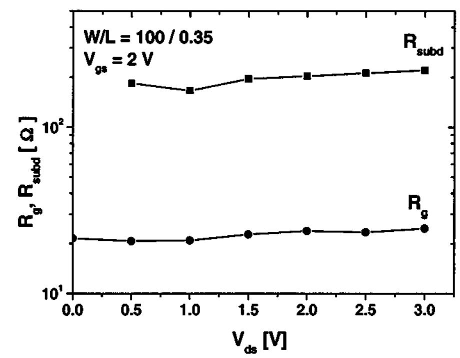

(b)

Fig. 7. Drain-bias dependence of small-signal parameters for an n-MOSFET having 100-μm width and biased to $V_{\rm gs} = 2$ V. (a) Capacitances. (b) R_g and $R_{\rm subd}$.

The gate-bias dependences of extracted capacitances is shown in Fig. 6(a). $C_{\rm gs}$ and $C_{\rm gd}$ are composed of the intrinsic components $C_{\rm gsi}$ and $C_{\rm gdi}$ and the overlap components $C_{\rm gso}$ and $C_{\rm gdo}$. In the saturation region, intrinsic capacitances $C_{\rm gdi}$ and $C_{\rm sd}$ are almost zero because the drain voltage does not influence the device charges. The total gate-to-drain capacitance $C_{\rm gd}$ is dominated by the overlap capacitance $C_{\rm gdo}$. As gate bias increases for constant $V_{\rm ds}$, $C_{\rm gd}$ and $C_{\rm dg}$ increase due to an increase of the intrinsic capacitance. $C_{\rm gs}$ and C_m increase with $V_{\rm gs}$ near the threshold voltage at the onset of the strong inversion region and are almost constant in the strong inversion saturation region.

The extracted R_g and $R_{\rm subd}$ with gate bias are shown in Fig. 6(b) and they are almost constant with gate bias in the strong inversion region.

In Fig. 7, drain-bias dependence of the extracted small-signal parameters for the n-MOSFET biased to $V_{\rm gs} = 2$ V is shown. The drain-bias dependence of extracted capacitance is shown in Fig. 7(a). The vertical line at $V_{\rm ds} = 0.81$ V is the boundary between the linear and saturation regions. The transistor is biased in the linear region with low $V_{\rm ds}$, The intrinsic behavior of the transistor becomes symmetric in terms of drain and source. Thus, the intrinsic capacitances $C_{\rm gsi}$ and $C_{\rm gdi}$ are almost the same at $V_{\rm ds} = 0$ V. In Fig. 7(a), the difference between $C_{\rm gs}$ and $C_{\rm gd}$ at $V_{\rm ds} = 0$ V is due to the parasitic $C_{\rm gb}$, which is included in the $C_{\rm gs}$. $C_{\rm gb}$ of the gate contact pad component and poly-to-well capacitance in the field oxide becomes the major part of the parasitic capacitance. At $V_{\rm ds} = 0$ V, $C_{\rm dg}$ is the same as $C_{\rm gd}$ and $C_m = 0$. C_m increases with a $V_{\rm ds}$ increase in the linear region and is almost constant for high $V_{\rm ds}$ in the saturation region. $C_{\rm sd}$ becomes negative in the linear region because raising the drain voltage will increase the effective reverse bias at the drain end and will cause the magnitude of the inversion layer charges to decreases. In the saturation region for higher $V_{\rm ds}$, gate-to-drain capacitance $C_{\rm gd}$ is almost the same as $C_{\rm gdo}$.

The extracted capacitance parameters correctly model the bias dependence of the intrinsic capacitance. Since the conventional *CV* measurements using a large *CV* test structure are less sensitive to extract small capacitance values in short-channel microwave MOSFETs, measuring S-parameters of microwave MOSFETs themselves in the high-frequency range of gigahertz is better than conventional *CV* measurements. The proposed parameter-extraction method can be applied to accurate intrinsic capacitance modeling at the gigahertz operation. Extracted R_g and $R_{\rm subd}$ with drain bias are shown in Fig. 7(b) and they are almost constant with drain bias.

In Fig. 8, g_m and $g_{\rm ds}$ extracted from the S-parameter measurement and those obtained from dc measurement are compared. Extracted g_m and $g_{\rm ds}$ as a function of $V_{\rm gs}$ with gate bias for $V_{\rm ds} = 2$ V are shown in Fig. 8(a) and extracted g_m and $g_{\rm ds}$ as a function of $V_{\rm ds}$ with drain bias for $V_{\rm gs} = 2$ V are shown in Fig. 8(b). They match very well with each other, verifying the validity of the extraction method. The extraction results correctly modeled the bias dependence of g_m and $g_{\rm ds}$ in the linear and saturation regions.

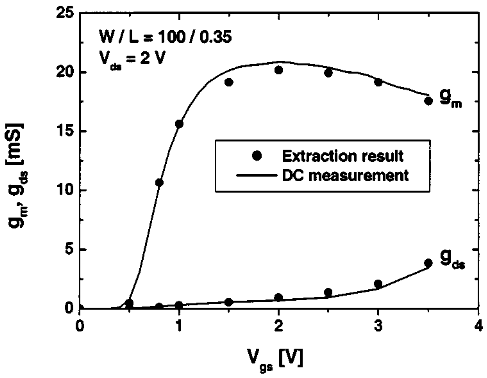

(a)

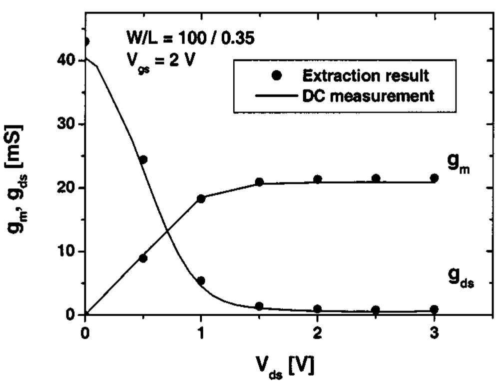

(b)

Fig. 8. (a) Extracted g_m and $g_{\rm ds}$ with gate bias for $V_{\rm ds} = 2$ V. (b) Extracted g_m and $g_{\rm ds}$ with drain bias for $V_{\rm gs} = 2$ V. g_m and $g_{\rm ds}$ extracted from the S-parameter measurement and those obtained from dc measurement are compared.

For a conventional *I–V* model, g_m and $g_{\rm ds}$ are derived by differentiating $I_{\rm ds}$. Although $I_{\rm ds}$ fit well with the measurements, the slope may have large errors. This can have very serious consequences in analog circuit design. The proposed extraction method from S-parameters can directly extract the conductances g_m and $g_{\rm ds}$ without differentiation, and these results are more accurate.

IV. Conclusion

A novel direct extraction method for obtaining accurate high-frequency small-signal parameters for a MOSFET including substrate-related parameters and nonreciprocal capacitors has been demonstrated. The extracted results are physically meaningful and good agreement has been obtained between the simulation results of the equivalent circuit and measured data without any optimization. The extracted parameters, such as g_m and $g_{\rm ds}$, also match very well with those obtained by dc measurement.

References

[1] G. Dambrine, A. Cappy, F. Helidore, and E. Palyze, "A new method for determining the FET small-signal equivalent circuit," *IEEE Trans. Microwave Theory Tech.*, vol. 36, pp. 173–176, July 1998.

[2] B. L. Ooi, M. S. Leong, and P. S. Kooi, "A novel approach for determining the GaAs MESFET small-signal equivalent-circuit element," *IEEE Trans. Microwave Theory Tech.*, vol. 45, pp. 2084–2088, Oct. 1993.

[3] W. Liu, R. Gharpurey, M. C. Chang, U. Erdogan, R. Aggarwal, and J. P. Mattia, "RF MOSFET modeling accounting for distributed substrate and channel resistance with emphasis on the BSIM3v3 SPICE model," in *IEEE Electron Devices Meeting Tech. Dig.*, Dec. 1997, pp. 309–312.

[4] J. J. Ou, X. Jin, I. Ma, and C. Hu, "CMOS RF modeling for GHz communication IC's," in *IEEE Very Large Scale Integration Symp. Tech. Dig.*, June 1998, pp. 94–95.

[5] D. R. Pehlke, M. Schroder, A. Burstein, M. Matloubian, and M. F. Chang, "High frequency application of MOS compact model and their development for scalable RF model libraries," in *Proc. Custom Integrated Circuits Conf.*, May 1998, pp. 219–222.

[6] R. Sung, P. Bendix, and M. B. Das, "Extraction of high-frequency equivalent circuit parameters of submicrometer gate-length MOSFETs," *IEEE Trans. Electron Devices*, vol. 45, pp. 1769–1775, Aug. 1998.

[7] C. H. Kim, C. S. Kim, H. Y. Yu, and K. S. Nam, "Unique extraction of substrate parameters of common-source MOSFETs," *IEEE Microwave Guided Wave Lett.*, vol. 9, pp. 108–110, Mar. 1999.

[8] P. Yang, B. D. Epler, and P. K. Chatterjee, "An investigation of the charge conservation problem for MOSFET circuit simulation," *IEEE J. Solid-State Circuits*, vol. SSC-18, pp. 128–138, Feb. 1983.

[9] Y. Tsividis, *The Operation and Modeling of the MOS Transistor*. New York: McGraw-Hill, 1987.

[10] X. Jin, J. J. Ou, C.-H. C, W. Liu, J. Deen, P. R. Gray, and C. Hu, "An effective gate resistance model for CMOS RF and noise modeling," in *IEEE Electron Devices Meeting Tech. Dig.*, 1998, pp. 961–964.

[11] C. E. Biber, M. L. Schmatz, T. Morf, U. Lott, and W. Bachtold, "A nonlinear microwave MOSFET model for spice simulators," *IEEE Trans. Microwave Theory Tech.*, vol. 46, pp. 604–610, May 1998.

Ickjin Kwon (S'00) was born in Korea, on March 13, 1976. He received the B.S. and M.S. degrees in electrical engineering and computer science from the Korea Advanced Institute of Science and Technology (KAIST), Taejon, Korea, in 1998 and 2000, respectively, and is currently working toward the Ph.D. degree at KAIST.

His current research interests include CMOS RF circuits and modeling.

Mr. Kwon was the recipient of the Samsung Paper Award presented at the 2001 Korean Conference on Semiconductors.

Minkyu Je (S'97) was born in Korea, on January 23, 1975. He received the B.S. and M.S. degrees in electrical engineering and computer science from the Korea Advanced Institute of Science and Technology (KAIST), Taejon, Korea, in 1996 and 1998, respectively, and is currently working toward the Ph.D. degree in electrical engineering and computer science at KAIST.

His current research interests include CMOS RF modeling and RF circuits.

Mr. Je received the second place award of the 1998 IEEE Region 10 Post Graduate Student Competition.

Kwyro Lee (S'79–M'80–SM'90) received the B.S. degree in electronics engineering from the Seoul National University, Seoul, Korea, in 1976, and the M.S. and Ph.D. degrees from the University of Minnesota at Minneapolis–St. Paul, in 1979 and 1983, respectively.

While with the University of Minnesota at Minneapolis–St. Paul, he was involved with many pioneering research of modeling heterojunction field-effect transistors. From 1983 to 1986, he was an Engineering General Manager with GoldStar Semiconductor Inc., Gumi, Korea, where he was responsible for the development of the first polysilicon CMOS products in Korea. In 1987, he joined the Korea Advanced Institute of Science and Technology (KAIST) as an Assistant Professor in the Department of Electrical Engineering and Computer Science, and where he is currently a Professor. Since 1997, he has also been the Director of the Micro Information and Communication Remote-Object Oriented Systems (MICROS) Research Center. His research interests are focused on RF and baseband circuits for mobile multimedia. He co-authored *Semiconductor Device Modeling for VLSI* (Englewood Cliffs, NJ: Prentice-Hall, 1993).

Dr. Lee is a life member of the Institute of Electronics Engineers of Korea (IEEK). He served as the chairman of the IEEE Korea Electron Device Chapter and as a Technical Committee member at the IEEE International Electron Devices Meeting (1997–1998).

Hyungcheol Shin (S'92–M'9–SM'00) received the B.S. degree (*magna cum laude*) and the M.S. degree in electronics engineering from the Seoul National University, Seoul, Korea, in 1985 and 1987, respectively, and the Ph.D. degree in electrical engineering from the University of California at Berkeley, in 1993.

From 1994 to 1996, he was with Motorola Advanced Custom Technologies, where he was a Senior Device Engineer. In 1996, he joined Department of Electrical Engineering and Computer Science, Korea Advanced Institute of Science and Technology (KAIST), Taejon, Korea, as an Assistant Professor and where he is currently an Associate Professor. His current research interests include nano-CMOS, CMOS RF modeling, and RF circuits. He has authored or co-authored over 140 technical papers in international journals and conference proceedings and also authored one chapter in a Japanese book on plasma charging damage. He is listed in Marquis's *Who's Who in the World*, *The Outstanding People of the 20th Century-Second Edition*, and the *International Personality of the Year*.

Prof. Shin is a life member of the Institute of Electronics Engineers of Korea (IEEK). He has served as a committee member of several international conferences, including the IEEE Silicon Nanoelectronics Workshop and the IEEE Symposium on Plasma-Process Induced Damage (P2ID). He was the recipient of the 1991 Second Best Paper Award presented by the American Vacuum Society, the 1998 Excellent Teaching Award presented by the Department of Electrical Engineering and Computer Sciences, KAIST, and the 1999 Haedong Paper Award presented by IEEK.